

# Prediction of Wood Elastic Strain Development Trend in Conventional Drying Process Based on GM-BP Model

Wanhui Gao,<sup>a</sup> Jingyao Zhao,<sup>a</sup> Xiaodong Zhu,<sup>a</sup> Dongyan Zhou,<sup>b</sup> Liangyan Guo,<sup>a</sup> and Yingchun Cai<sup>a,\*</sup>

The elastic strain of wood reflects the nature (stretching or compression) and the magnitude of the drying stress at that time during the conventional drying process. The accurate prediction of strain is important to optimize the drying process and to improve drying speed and quality. In this work, the elastic strain was measured in real time, and moisture content was measured by periodic weighing during the drying process. Using these data, the GM (1,1) grey prediction model was used to predict moisture content in adjacent periods in the future. Based on the moisture content predicted by GM (1,1), a BP neural network was constructed to predict the development trend of elastic strain in the surface layer and core layer. The prediction results of the GM-BP combination model showed that the fitting error range of the prediction of the surface layer elastic strain was  $[-5 \times 10^{-3} \sim 5 \times 10^{-3}]$ , with a mean square error (MSE) of  $2.31 \times 10^{-7}$ . The elastic strain of the core layer was  $[-2 \times 10^{-3} \sim 2 \times 10^{-3}]$ , and the MSE was  $3.86 \times 10^{-8}$ . Thus, the GM-BP model achieved high accuracy for predicting the development trend of elastic strain. It can provide a new method and innovative thinking for the optimization and control of wood drying process.

*Keywords:* Conventional wood drying; Grey prediction model; BP neural network; Elastic strain; Development tendency

*Contact information:* a: Key Laboratory of Bio-Based Material Science & Technology (Northeast Forestry University), Ministry of Education, Harbin, China 150040; b: China Jiliang University, Hangzhou, China 310000; \* Corresponding author: caiyingchunnefu@163.com

## INTRODUCTION

Drying stress is the main cause of defects in dry wood (Fu *et al.* 2013). It is an important basis for formulating and reliably implementing drying process standards and is a key factor for ensuring the drying quality of wood. Therefore, the rapid and accurate prediction of drying stress has become an area of research emphasis, particularly in detection methods and simulation. Detection mainly involves the slice method, sound emission method (Booker and Doe 1995), optical methods, the strain gage method (Cheng 2007), and digital image analytical methods of measuring (Jeong *et al.* 2009; Peng *et al.* 2011). These methods test the drying stress, but unless the precision of the results is improved, such tests cannot achieve detection online. Simulation has mainly used a BP artificial neural network to predict the drying stress that is generated at a specific moment where external parameters of drying stress are input (Fu *et al.* 2017), but this method cannot be used to predict the development and change in drying stress in the next moment. The generation and development of drying stress are dynamic parameters that change with time (drying process) and are affected by the temperature and humidity of the external environment, the wood self-shape, and the moisture content (Chai *et al.* 2019). Specifically, the change trend for drying stress is a multi-factor and dynamic nonlinear time series

function with drying time. Therefore, establishing a development trend prediction model with time of drying stress has important practical significance for achieving real-time monitoring and subsequently adjusting the benchmarks of the drying process, controlling drying stress, and improving drying quality.

Artificial neural networks are often able to make accurate predictions for nonlinear complex systems on account of their strong organizational integration ability (Poonnoy and Tansakul 2007), and they are used to establish mathematical models that reflect the internal relationship of experimental data after finite iterative calculations of acquired experimental data (Rai *et al.* 2005). The artificial neural networks used in simulating the time series are mainly the BP neural network and the LSTM neural network (Ma *et al.* 2015). The BP neural network can be used for the time series to predict the preceding one or more values in a series based on the current values. This method ignores the influence of external parameters on predictions, and it certainly lacks a theoretical basis and foundation. Thus, the predicted result has certain error. The LSTM neural network is used for predicting time series, and it usually requires a large amount of data (Liu *et al.* 2018). The data are predicted with some regularity and are cyclical. However, the benchmark for wood drying strain involves artificial external parameters or the process to produce drying strain is under different processes, each of which is not identical. Thus, there is a lack of regularity. Therefore, these two methods are not suitable for predicting time series of drying strain, and this makes it difficult to predict the drying strain time series of wood. The GM (1,1) is mainly used for small samples, and no obvious change rule of the data has good predictive power (Zhou and He 2013). The GM (1,1) was used to predict the development trend of moisture content in adjacent periods in the future, and the BP neural network has the characteristics of a higher fitting degree of historical data. Thus, the GM-BP are combined to achieve prediction of development trend of wood drying elastic strain in adjacent periods in the future. The artificial neural network approach has been widely used in the field of wood drying (Ceylan and İhan 2008; Chai *et al.* 2018), but the research on its combination with the time series has not yet been reported. Therefore, a predictive model for the wood drying strain time series with multi-data fusion is established using a time series combined with the GM-BP model to achieve real-time detection and accurate prediction of wood drying strain. At the same time of the wood drying strain, the elastic strain corresponds to the drying stress at that time, and the elastic strain can reflect the drying stress. The wood drying stress of the surface and core layers has a significant impact on the crack. When the stress of the surface and core layers exceed the transverse tensile strength of the wood, wood tends to form cracks. Therefore, it is necessary to focus on predicting the elastic strain of the surface and core.

In this work, 45-mm thick Mongolian pine served as the object. Some data were measured in real time online, and moisture content changing with time was measured by periodic weighing during drying process. The GM-BP combination model was used to simulate development trend of the elastic strain of the surface and core layers of wood during the wood drying process. Based on the moisture content predicted by GM (1,1) model and drying medium temperature, humidity and wood position corresponding to the moisture content in the selected drying benchmark, a BP neural network was constructed to predict the development trend of elastic strain in the surface layer and core layer in adjacent periods in the future (the above model is referred to as GM-BP model). The research purpose is to explore an accurate predictive model of development trends of the elastic strain of the surface and core layers *via* assessing the feasibility and accuracy of the model using network training and validation.

## EXPERIMENTAL

### Materials and Equipment

Mongolian pine with an initial moisture content of 56.4% was processed into samples that had dimensions of 140 mm (T) × 45 mm (R) × 500 mm (L). Mongolian pine were obtained from the Greater Khingan Range forest area.

The drying equipment consisted of a constant temperature and humidity chamber (DS-100) from Xinda experimental equipment Co. Ltd. (Suzhou, China). The inside dimension of the chamber was 1000 mm × 1000 mm × 800 mm. The HYD-ZS wood moisture content on-line detection instrument was purchased from Yuda Electronic Technology Co. Ltd. (Heilongjiang, China).

### Methods

#### Parameter detection

The process method and drying process data are shown in Table 1. After a preheating treatment, HYD-ZS was used to measure the average moisture content of test material by inserting the probe of HYD-ZS into 1/2 of the wood thickness, and the probe spacing was about 30 mm. The test material for strain detection was taken out to cut a strain specimen (10 mm in fiber direction) every 4 h. Then silicone was used to seal the truncated end part to ensure that axial moisture transfer does not occur. The specimen was then put back into the drying oven to continue drying. The strain specimen was decomposed into strain slices with a thickness of 5 mm. The sawing method is shown in Fig. 1. A digital camera was used to collect the length images of the strain slices of the surface layer and the core layer before and after the decomposition (shot with the scale at the same time). The current length of the strain slices was analyzed by ImageJ software (<https://imagej.nih.gov/ij/>), and after dried every 4 h, by sliced the way the variation of elastic strain before and after sliced was calculated using Eq. 1,

$$\varepsilon_e = \frac{L_1 - L_2}{L_0} \quad (1)$$

where  $L_0$  is the distance between two measuring points of the strain slice before drying,  $L_1$  is the distance between two measuring points of the strain slice before sawing, and  $L_2$  is the distance between two measuring points of the strain slice immediately after the sample was sawed along the line.

After the strain specimen was decomposed, the strain slices of 9 layers were immediately weighed, marked as  $G_i$ , where  $i$  is the layer number. After image acquisition, the strain slices of each layer were dried, and the absolute dry weight was denoted as  $G_{0i}$ . The average moisture content was calculated using Eq. 2 (Cai *et al.* 2005),

$$\bar{W} = \frac{\sum_{i=1}^9 G_i - \sum_{i=1}^9 G_{0i}}{\sum_{i=1}^9 G_{0i}} \times 100 \quad (\%) \quad (2)$$

where  $G_i$  is the moisture content corresponding to the strain slices of 9 layers immediately weighed after the strain specimen was decomposed.  $G_{0i}$  is the moisture content that was the absolute dry weight of the strain slices weighed.

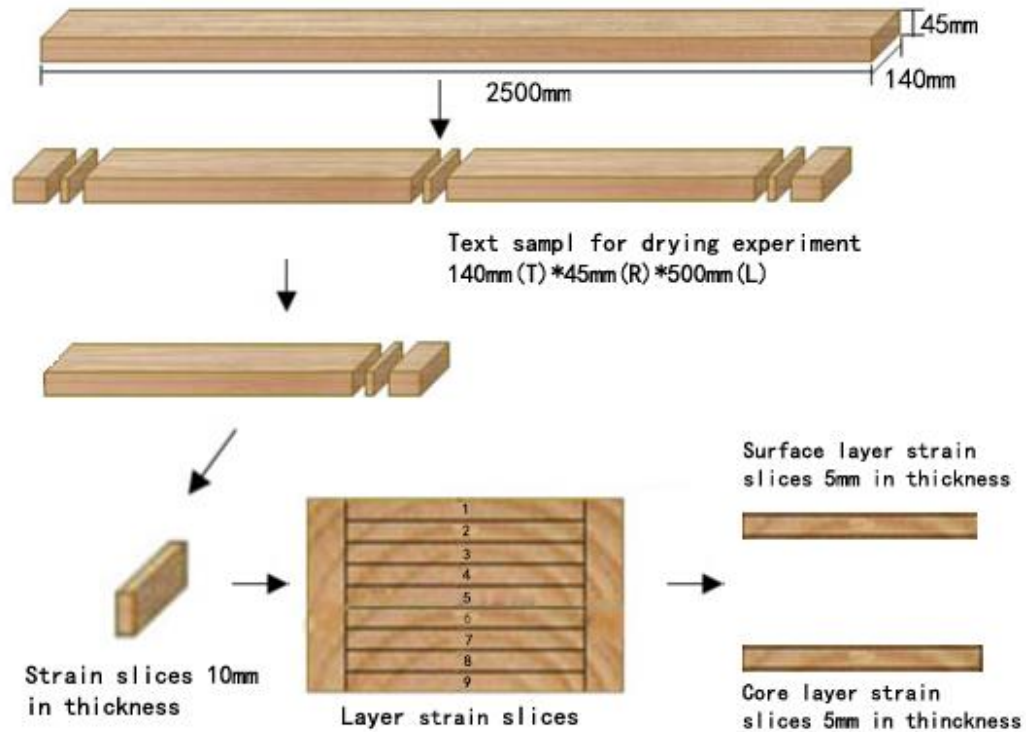


Fig. 1. Schematic diagram of the strain slice sawed of Mongolian pine

Table 1. Drying Standards of Mongolian Pine

Moisture Content (%)	Dry Bulb Temperature (°C)	Wet Bulb Temperature (°C)	Equilibrium Moisture Content (%)
>40	60	56	15
40 - 30	62	57	14
30 - 25	65	57	13
25 - 20	68	58	11
20 - 15	70	57	9
15 - 10	73	58	7
< 10	76	56	6

GM (1,1) Grey prediction model

The GM (1,1) mainly uses the presented dynamic development trend to predict the future trend of data *via* differential equation fitting of the original data and an infinite approximation of the sequence of number (Wu 2019). The model has good predictive power for data with a few samples and no obvious pattern. The prediction process is as follows.

The original sequence is  $X^{(0)} = [x^0(1), x^0(2), \dots, x^0(n)]$ , where  $x^0(k) \geq 0$  ( $k = 1, 2, \dots, n$ ). A summation of the original sequence yields a new sequence:  $X^{(1)} = [x^1(1), x^1(2), \dots, x^1(n)]$ . The first order differential equation is applied to the sum sequence. The GM (1,1) model is expressed as follows:

$$\frac{dx^{(1)}}{dt} + ax^{(1)} = b \tag{3}$$

where  $a$  is the development parameter and  $b$  is the grey action quantity.

When  $|a| < 2$ , the GM (1,1) is meaningful. The value is determined by the least squares method,  $[a, b]^T = (B^T B)^{-1} B^T Y$ , where B and Y are known matrices and their expressions are as follows (Wu *et al.* 2014).

$$B = \begin{bmatrix} -\frac{1}{2}[x^{(1)}(2) + x^{(1)}(1)] & 1 \\ -\frac{1}{2}[x^{(1)}(3) + x^{(1)}(2)] & 1 \\ \vdots & \vdots \\ -\frac{1}{2}[x^{(1)}(n) + x^{(1)}(n-1)] & 1 \end{bmatrix} \quad Y = \begin{bmatrix} x^{(0)}(2) \\ x^{(0)}(3) \\ \vdots \\ x^{(0)}(n) \end{bmatrix} \quad (4)$$

When the calculated values of a and b are substituted into the above differential equation, the time response function is obtained as Eq. 5.

$$\hat{x}^{(1)}(t+1) = \left[ x^{(0)}(1) - \frac{b}{a} \right] e^{-at} + \frac{b}{a} \quad (5)$$

When the derivative of Eq. 5 is reduced, the predictive equation is obtained as Eq. 6.

$$\hat{x}^{(0)}(t+1) = a \left[ x^{(0)}(1) - \frac{b}{a} \right] e^{-at} \quad (6)$$

The performance of the GM (1,1) is evaluated *via* residual testing and posterior testing. The fitting degree and predictive accuracy of the model are also evaluated via residual testing and posterior residual testing.

For the residual testing, the original sequence is  $x^{(0)}(t)$ . The predicted sequence is  $\hat{x}^{(0)}(t)$ , and the residual is  $\varepsilon(t) = x^{(0)}(t) - \hat{x}^{(0)}(t)$ . The relative error is  $\Delta(t) = \left| \frac{\varepsilon(t)}{x^{(0)}(t)} \right|$ . When  $\Delta(t) < 0.2$ , model accuracy is qualified.

For the posterior residual testing: the posterior residual C is the ratio of two variances. Specifically, the ratio is  $C = \frac{S_2}{S_1}$ , where  $S_1^2 = \frac{1}{n} \sum_{t=1}^n [x^{(0)}(t) - \bar{x}]^2$  and  $S_2^2 = \frac{1}{n} \sum_{t=1}^n [\hat{x}^{(0)}(t) - \bar{\hat{x}}]^2$ . The term  $\bar{x}$  is the average  $x^{(0)}(t)$ , and  $\bar{\varepsilon}$  is the average  $\varepsilon(t)$ . The probability of minimum error is  $P = P\{|\varepsilon(t) - \bar{\varepsilon}| < 0.6754S_1\}$ . The data verify the validity and the predicted effect of the model in Table 2 (Li *et al.* 2011).

**Table 2.** Prediction Accuracy Level of the Model

P	C	Model accuracy
>0.95	<0.35	Good
>0.80	<0.50	Qualified
>0.70	<0.65	Barely qualified
<0.70	>0.65	Unqualified

#### BP Neural network prediction model

The BP neural network mainly involves an input layer, hidden layer, and output layer (Watanabe *et al.* 2014). The topology of the BP neural network is constructed by connecting the hidden layers. The input layer and hidden layer are activated *via* a tangent Sigmoid function, and the hidden layer and output layer are connected *via* a linear function (Watanabe 2013). The neuron number of predictive models have a significant impact, and the neuron nodes are estimated according to the actual need in the input layer and output

layer. The rule for the number of the neuron nodes does indeed require constant training the hidden layer. If there are too many nodes, the network training time increases and also leads to excessive fitting. If the node number is too few, the model training is inadequate, and the model cannot express the relationship between input variables and output parameters. Thus, determining the number of hidden layer nodes is a key to the predictive ability of the entire network model.

The performance of the BP neural network model was tested. Samples were used to train the model. The determining coefficient  $R^2$  and the mean squared error (MSE) was determined to evaluate the model. The formulas for calculating  $R^2$  and MSE are as follows,

$$R^2 = \frac{\sum_{i=1}^n (t_i - p_i)^2}{\sum_{i=1}^n t_i^2 \sum_{i=1}^n p_i^2} \quad (7)$$

$$Mse = \frac{1}{n} \sum_{n=1}^n (t_i - p_i)^2 \quad (8)$$

where  $n$  represents the number of groups of data,  $t_i$  is the test value, and  $p_i$  is the predicted value. The value of  $R^2$  is within  $[0,1]$ . When the value is closer to 1, the performance of the model is better. When the MSE value is smaller, the prediction performance is better. The learning efficiency is set at 0.01.

## RESULTS AND DISCUSSION

### Time Series Analysis of Elastic Strain in Surface and Core Layers

The elastic strain of the sample surface layer and core layer was measured every 4 h according to the benchmark of drying set. The variation trend of the elastic strain with the time series is shown in Figs. 2 and 3.

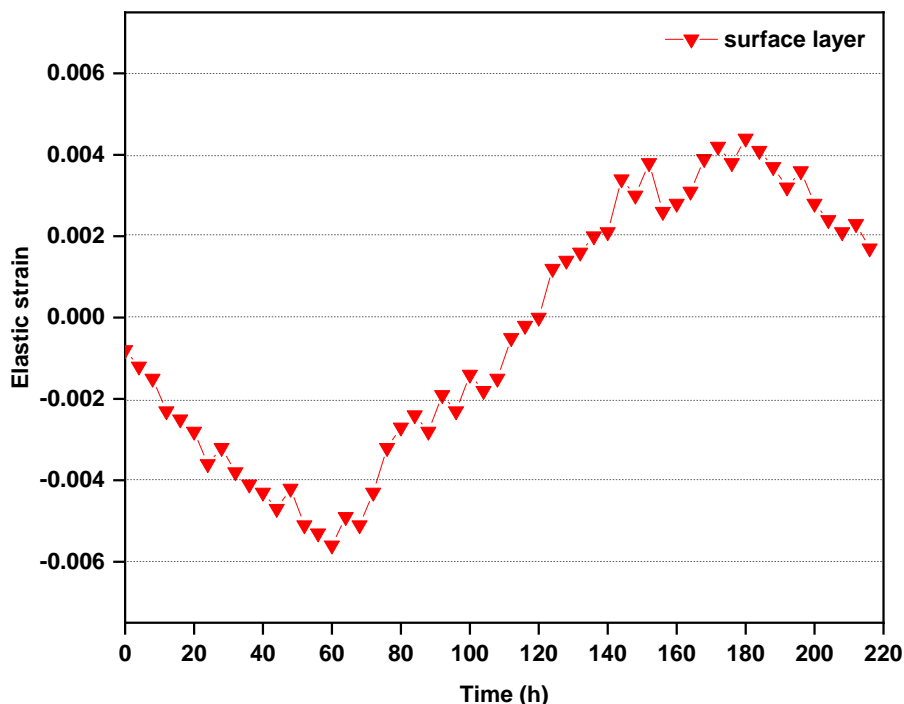
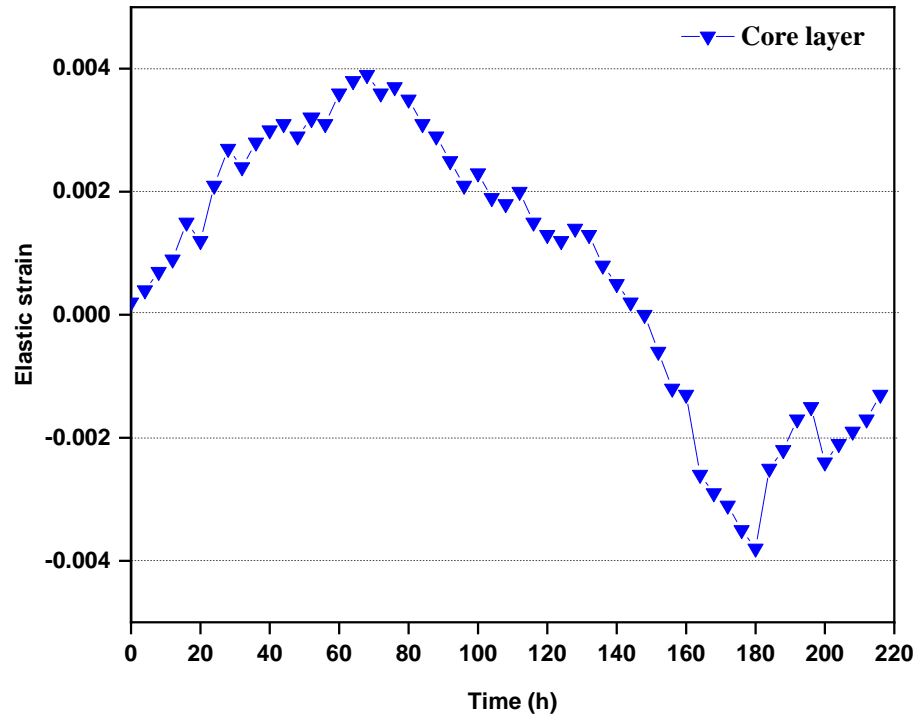


Fig. 2. Distribution of elastic strain of the surface layer



**Fig. 3.** Distribution of elastic strain of the core layer

In the early stage of the drying to about 60 h, the tensile elastic strain of the surface layer increases gradually due to the action of the tensile stress from the core layer with the decrease of moisture content (Zhan *et al.* 2009). With the drying process to about 180 h, mechanical adsorption creep occurs in the surface layer under the action of tensile stress, and this causes the tensile stress of the surface layer to be restrained and gradually to decrease due to the influence of plastic deformation. Correspondingly, the compressive stress of the core layer also decreases. When the core continues to shrink in the middle and later stages of drying, shrinkage of the surface inhibits shrinkage of the core. This transforms compressive stress of the core to tensile stress to achieve a change in stress, and this tendency gradually increases in the reverse direction. Meanwhile, the stress from the surface layer also transforms from tensile stress to compressive stress and increases with further drying. When dried for 180 h to the end, under the action of tensile mechanical adsorption creep from the core layer, the tensile stress of the core layer begins to decrease, and in response to the surface compression stress begins to decrease.

### Prediction Analysis of the GM (1,1)

The GM (1,1) is used to predict development trend of the main external parameters that affect the drying strain of wood. The main external parameters of the drying strain of wood include drying temperature, drying humidity, moisture content, and the location of the surface layer and the core layer (Fu *et al.* 2014). The moisture content also determines the temperature and humidity of the drying medium, and the prediction of the development trend of the next stage in the drying process. Thus, it is necessary to establish the GM (1,1) prediction for moisture content to predict the development trend of moisture content in adjacent periods in the future. The specific method is to make use of part of the data of moisture content changing with time, which was measured online in real time during conventional drying process and measured by periodic weighing.

The GM (1,1) was established and simulated in MATLAB. After repeated trainings, the experimental values and predicted values obtained are shown in Fig. 4. After calculation, the model development coefficient  $a$  is  $-0.0298$ . Because of  $|a| < 2$ , the model prediction is meaningful. The Grey action quantity  $b$  is  $48.06$ , and the average relative error  $\Delta(t)$  is  $1.27\%$ , where  $\Delta(t) < 0.2$ . This indicates that the model accuracy is qualified. The posterior residual  $C$  is  $0.2012 < 0.35$ , and the error probability is small ( $P=1$ ). According to the comparison shown in Table 2, the model has a high accuracy, with a grade of 1, and this indicates that the GM (1,1) has high accuracy in predicting the development trend of moisture content in adjacent periods in the future.

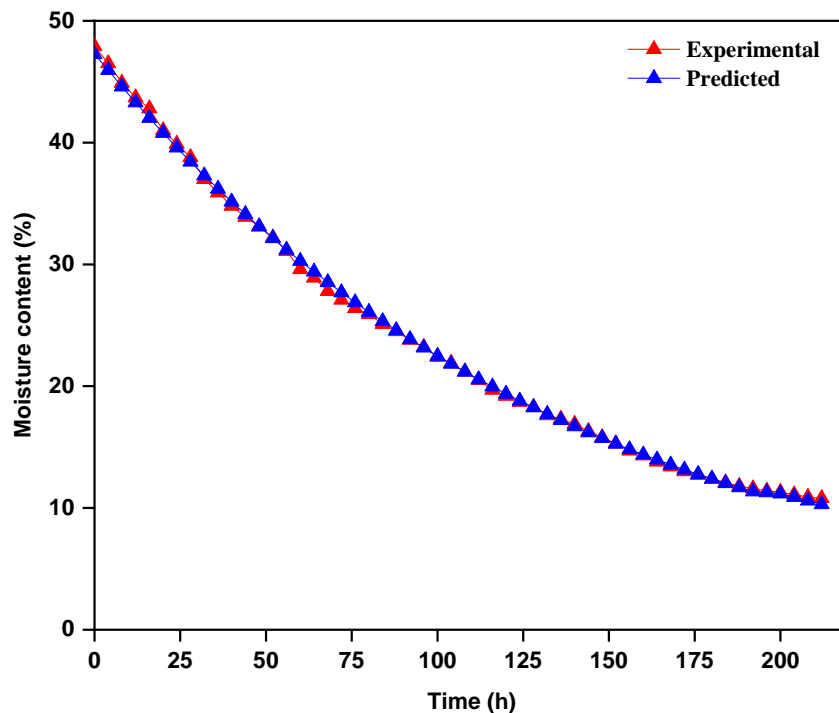


Fig. 4. Comparison of experimental and predicted moisture content using the GM (1,1) model

### Prediction Analysis of the GM (1,1)-BP

The BP neural network model was established in MATLAB. Based on the four main external influence parameters of wood drying strain, *i.e.*, temperature, humidity of drying medium on drying basis, moisture content, and the location of the surface and the core layer, these four parameters were selected as variables of the input layer. Because the input and output parameters were relatively simple in this study, to improve the training speed, a single hidden layer was chosen. A different number of neurons was used to train the network. When the number of hidden layer neurons was 5, the error of the neural network training was a minimum, and the network training speed was fast. Therefore, a 4-5-1 topological structure of neural network model was constructed. All data were randomly divided into training groups, a verification group, and a testing group. The training group accounted for 60% of the total data, and the verification group and testing group accounted for 20% each. Figure 5 shows the BP neural network training regression plots of the training group, verification group and testing group. The determined coefficient  $R^2$  for each training set is above 98%. This result was consistent with the determination coefficient  $R^2$  of all data sets higher than 0.956 by using artificial neural network to predict elastic strain,



taking drying temperature, water content, relative humidity and distance from the core as input variables in Fu's study (Fu *et al.* 2017), which indicates that the experimental value and the predicted value agree well. According to the preliminary assessment, the BP neural network model can be used to simulate and predict the elastic strain changes of the surface layer and core layer.

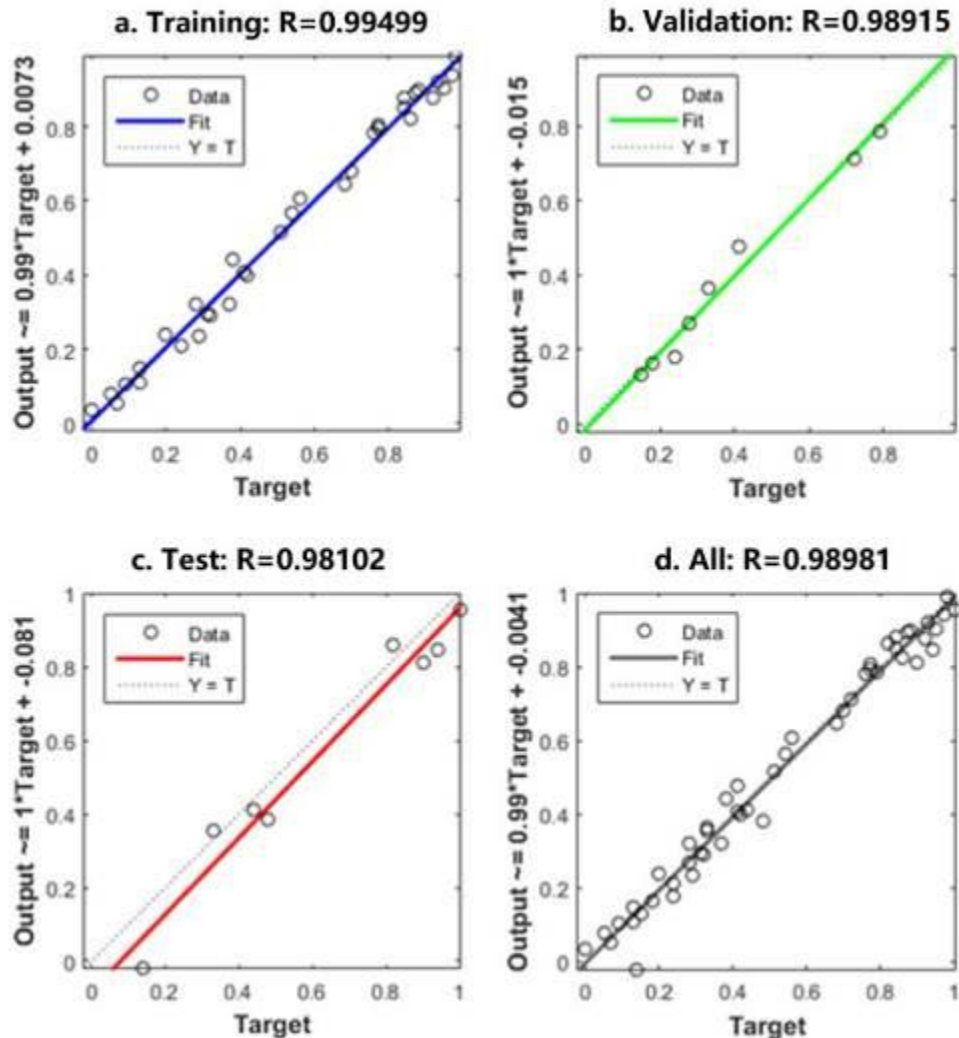


**Fig. 5.** Regression plots of the predicted values of the artificial neural network: (a) training sets, (b) verification set, (c) testing sets, and (d) aggregate data sets

The GM (1,1) was combined with BP neural network, that is, the GM (1,1) was used to predict development trend of moisture content. The drying temperature and drying humidity were determined according to the range of the predicted moisture content in the benchmark of drying set. The four variable input parameters were used in the established BP neural network. The elastic strain of the surface and core layers were simulated in adjacent periods in the future, and the predicted values and experimental values are compared in Figs. 6 and 7. The overall trend of the predicted value and the experimental value is consistent and close to that of the experimental value. The combined model of the GM (1,1) and BP neural network that is proposed in this study is an accurate and feasible method for predicting time series of the wood drying strain.

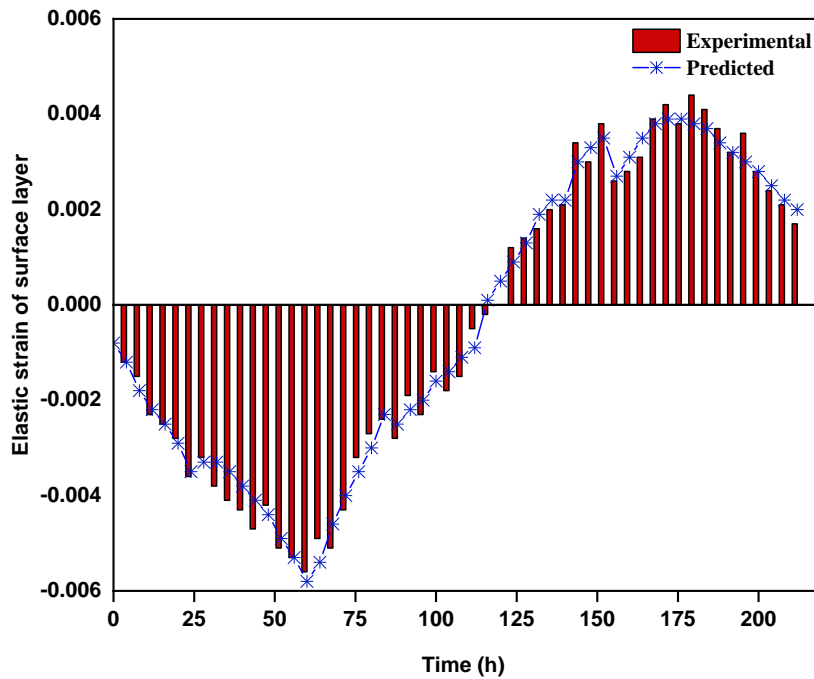


Fig. 6. Comparison of experimental and predicted surface elastic strain values

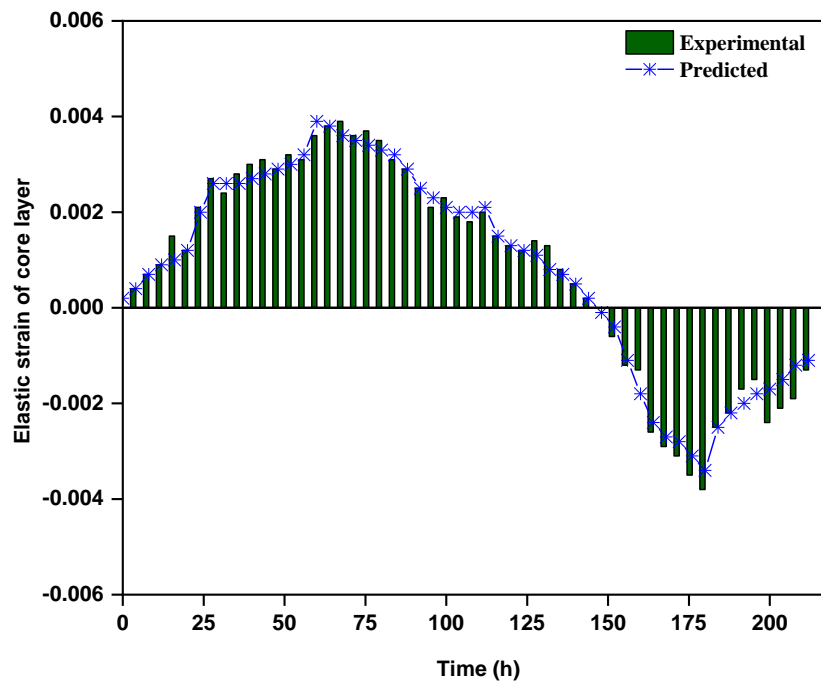


Fig. 7. Comparison of experimental and predicted values of elastic strain in the core layer

The error of the experimental and predicted elastic strain of the surface and core layers are shown in Figs. 8 and 9. The overall error of the surface elastic strain is concentrated between  $\pm 5 \times 10^{-3}$ , and the MSE is  $2.31 \times 10^{-7}$ . The overall error of the core elastic strain is concentrated between  $\pm 2 \times 10^{-3}$ , and the MSE is  $3.86 \times 10^{-8}$ . On the whole,

the predicted data reflected the development trend of elastic strain in adjacent periods in the future during the drying process, with low prediction error and high model accuracy. This model can be used for real-time monitoring and prediction and has important guiding value for subsequent adjustment of the process benchmark and control of drying stress and improvement of drying quality.

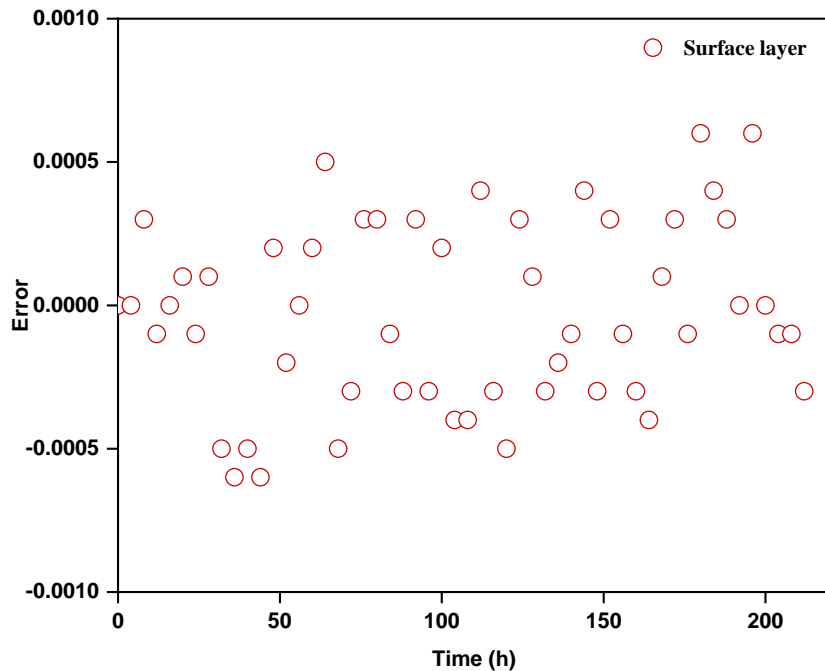


Fig. 8. Surface elastic strain prediction error

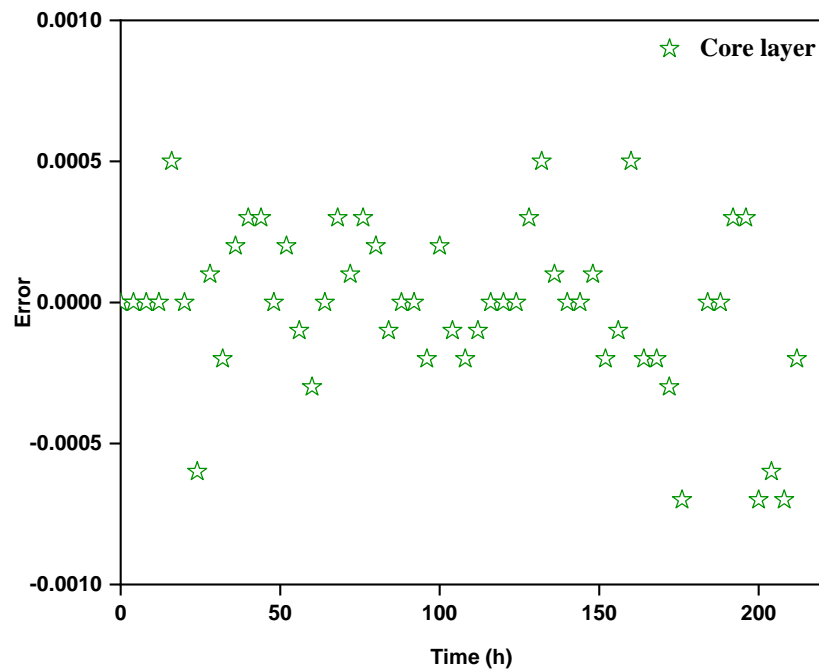


Fig. 9. Core elastic strain prediction error

## CONCLUSIONS

- 1 . Using the GM-BP combination model and real-time online measurement data, a model that combined the BP neural network and GM (1,1) was used to predict development trend of the elastic strain of the surface and core layers of wood during the wood drying process. The GM (1,1) has high accuracy in the development trend prediction of moisture content in adjacent periods in the future, and the accuracy level is 1.
- 2 . The drying temperature, drying humidity, moisture content, and the location of the surface and core layers are used as input variables to train the BP neural network. The value of  $R^2$  (the determined coefficient) of each training set is above 98%, and this indicates that the established BP neural network model can be used to predict the elastic strain of wood more accurately.
- 3 . The GM-BP are combined to achieve prediction of development trend of wood drying elastic strain in adjacent periods in the future. The results of the fitting error of the predicted development trend for the surface elastic strain in adjacent periods in the future are as follows: the range is  $[-5 \times 10^{-3} \sim 5 \times 10^{-3}]$ , and the MSE value is  $2.31 \times 10^{-7}$ ; the fitting error range of the predicted core layer elastic strain is  $[-2 \times 10^{-3} \sim 2 \times 10^{-3}]$ , and the MSE value is  $3.86 \times 10^{-8}$ . These values indicate that the GM-BP model that is proposed in this paper has high accuracy and practical value for simulating development trend for the elastic strain in adjacent periods in the future.

## ACKNOWLEDGMENTS

This work was financially supported by the Fundamental Research Funds for the National Natural Science Foundation of China (Grant No. 31670562) and the National Innovation Training Program for College Students of Northeast Forestry University (Grant No. 201910225018).

## REFERENCES CITED

- Booker, J. D., and Doe, P. E. (1995). "Acoustic emission related to strain energy during drying of *Eucalyptus regnans* boards," *Wood Science and Technology* 29(2), 145-156. DOI: 10.1007/BF00229344
- Cai, Y. C., Chen, G. Y., Ai, M. Y., and Sun, H. F. (2005). "Discussion on improving measurement accuracy of wood moisture content by oven drying method," *Journal of Beijing Forestry University* 27, 64-67.
- Chai, H. J., Zhao J. Y., and Cai Y. C. (2019). "Effects of pretreatment with saturated wet air and steaming on the high-frequency vacuum drying characteristics of wood," *BioResources* 14(4), 9601-9610. DOI: 10.15376/biores.14.4.9601-9610
- Chai, H. J., Chen, X., Cai Y. C., and Zhao J. Y. (2019). "Effects of pretreatment with saturated wet air and steaming on the high-frequency vacuum drying characteristics of wood," *Forests* 10(1), 16. DOI: 10.3390/f10010016
- Cheng, W. L. (2007). *Wood High Temperature and High Pressure Steam Drying Process Principle*, Science Press, Beijing, China.

- Ceylan, and İhan. (2008). "Determination of drying characteristics of timber by using artificial neural networks and mathematical models," *Drying Technology* 26(12), 1469-1476. DOI: 10.1080/07373930802412132
- Fu, Z. Y., Cai, Y. C., Zhao, J. Y., and Huan, S. Q. (2013). "The effect of shrinkage anisotropy on tangential rheological properties of Asian white birch disks," *BioResources* 8(4), 5235-5243. DOI: 10.15376/biores.8.4.5235-5243
- Fu, Z., Zhao, J. (2014). "Investigation of tangential strain caused by shrinkage anisotropy using image analytical method," *Engineering Sciences* 16(4), 25-29. DOI: 10.3969/j.issn.1009-1742.2014.04.005
- Fu, Z., Avramidis, S., Zhao, J., and Cai, Y. (2017). "Artificial neural network modeling for predicting elastic strain of white birch disks during drying," *European Journal of Wood and Wood Products* 75(6), 1-7. DOI: 10.1007/s00107-017-1183-x
- Jeong, G. Y., Zink-Sharp, A., and Hindman, D. P. (2009). "Tensile properties of earlywood and latewood from loblolly pine (*Pinus taeda*) using digital image correlation," *Wood & Fiber Science* 41(1), 51-63. DOI: 10.1145/1553374.1553534
- Li, J., Liao, R., and Chen, X. (2011). "Generalized accumulated GM(1,1) cosine model and its application," *Grey Systems Theory & Application* 2(2), 242-245. DOI: 10.1109/GSIS.2011.6044066
- Liu, J., Shahroudy, A., Xu, D., Kot, A. C., and Wang, G. (2018). "Skeleton-based action recognition using spatio-temporal LSTM network with trust gates," *IEEE Transactions on Pattern Analysis and Machine Intelligence* 40(12), 3007-3021. DOI: 10.1109/TPAMI.2017.2771306
- Ma, X. L., Tao, J. M., and Wang, Y. P. (2014). "Long short-term memory neural network for traffic speed prediction using remote microwave sensor data," *Transportation Research Part C: Emerging Technologies* 54(5), 187-197. DOI: 10.1016/j.trc.2015.03.014
- Peng, M. K., Chui, Y. H., Ho, Y. C., Wang, W. C., and Zhou, Y. T. (2011). "Investigation of shrinkage in softwood using digital image correlation method," *Applied Mechanics & Materials* 83, 157-161. DOI: 10.4028/www.scientific.net/AMM.83.157
- Poonnoy, P., and Tansakul, A. (2007). "Artificial neural network modeling for temperature and moisture content prediction in tomato slices undergoing microwave-vacuum drying," *Journal of Food Science* 72(1), 6. DOI: 10.1111/j.1750-3841.2006.00220.x
- Rai, P., Majumdar, G. C., Dasgupta, S., and De, S. (2005). "Prediction of the viscosity of clarified fruit juice using artificial neural network: a combined effect of concentration and temperature," *Journal of Food Engineering* 68(4), 527-533. DOI: 10.1016/j.jfoodeng.2004.07.003
- Watanabe, K. (2013). "Artificial neural network modeling for predicting final moisture content of individual Sugi (*Cryptomeria japonica*) samples during air-drying," *Journal of Wood Science* 59(2), 112-118. DOI: 10.1007/s10086-012-1314-2
- Watanabe, K., Kobayashi, I., Matsushita, Y., Saito, S., Kuroda, N., and Noshiro, S. (2014). "Application of near-infrared spectroscopy for evaluation of drying stress on lumber surface: A comparison of artificial neural networks and partial least squares regression," *Drying Technology* 32(5), 590-596. DOI: 10.1080/07373937.2013.846911
- Wu, J. L. (2019). "Study on GM(1,1) -BP neural network combination model based on grey relational grade," *Journal of Chongqing University of Technology* 33(11), 207-210.

- Wu, L. F., Liu, S. F., Cui, W., Liu, D. L., and Yao, T. X. (2014). “Non-homogenous discrete grey model with fractional-order accumulation,” *Neural Computing & Applications* 25(5), 1215-1221. DOI: 10.1007/s00521-014-1605-1
- Zhan, J. F., Gu, J., and Shi, S. Q. (2009). “Rheological behavior of larch timber during conventional drying,” *Drying Technology* 27(10), 1041-1050. DOI: 10.1080/07373930903218412
- Zhou, W., and He, J. M. (2013). “Generalized GM (1,1) model and its application in forecasting of fuel production,” *Applied Mathematical Modelling* 37(9), 6234-6243. DOI: 10.1016/j.apm.2013.01.002

Article submitted: April 11, 2020; Peer review completed: June 13, 2020; Revised version received and accepted: June 28, 2020; Published: July 2, 2020.  
DOI: 10.15376/biores.15.3.6371-6384